High-resolution temporal constraints on the dynamics of dark energy

Gong-Bo Zhao,[1,2] Dragan Huterer,[3] and Xinmin Zhang[2]

[1]*Department of Physics, Simon Fraser University, Burnaby, BC, V5A 1S6, Canada*
[2]*Institute of High Energy Physics, Chinese Academy of Science, P.O. Box 918-4, Beijing 100049, P. R. China*
[3]*Department of Physics, University of Michigan, 450 Church St., Ann Arbor, MI, 48109*

We use the recent type Ia supernova, cosmic microwave background and large-scale structure data to shed light on the temporal evolution of the dark energy equation of state $w(z)$ out to redshift one. We constrain the most flexible parametrization of dark energy to date, and include the dark energy perturbations consistently throughout. Interpreting our results via the principal component analysis, we find no significant evidence for dynamical dark energy: the cosmological constant model is consistent with data everywhere between redshift zero and one at 95% C.L.

Introduction. It has been recognized for some time now that accurate reconstruction of the expansion history of the universe is a crucial step towards understanding the physical mechanism behind the accelerating universe. Early work on constraining the expansion history had concentrated on parametrizing the equation of state (ratio of pressure to density) of dark energy $w(z)$ via one or two parameters and measuring them together with the energy density relative to critical Ω_{DE} [1–5]. More recently, the program of reconstructing the expansion history had been generalized to adding more parameters [6] and decorrelating them [7–9]. Nevertheless, the data at the time only allowed only up to three or four band-powers of $w(z)$ to be considered, leading to "jagged" expansion history, especially in the range $0.5 \lesssim z \lesssim 1$. In the future, a number of "principal components" of dark energy — parameters forming a natural basis in which the function $w(z)$ can be expanded — will be measured [10, 11].

In this paper, we utilize a new variant of the nearly model-independent approach to reconstruct $w(z)$ of dark energy with the latest astronomical observations including type Ia supernovae (SNe Ia), power spectra of the cosmic microwave background (CMB) anisotropies and galaxy distribution from the large-scale structure (LSS). We perform a full likelihood analysis using the Markov chain Monte Carlo approach [12], and make sure to properly take into account the dark energy perturbations [13]. Compared to previous work, our parametrization of the expansion history is more flexible and, as we argue, robust and easy to implement.

Method and Data. We consider the following cosmological parameter set

$$\{w_i, \omega_b, \omega_c, \Theta_s, \tau, n_s, \log[10^{10}A_s]\}, \qquad (1)$$

where $\omega_b \equiv \Omega_b h^2$ and $\omega_c \equiv \Omega_c h^2$ are the physical baryon and cold dark matter densities relative to critical, Θ_s is $100\times$ the ratio of the sound horizon to the angular diameter distance at decoupling, τ is the optical depth to re-ionization, A_s and n_s are the amplitude of the primordial spectrum and the spectral index respectively.

The remaining parameters, w_i ($i = 1, 2, ..n$), are the equation of state values at n specific fitting nodes $\{z_i\}$ — redshifts at which we vary these parameters indepen-

dently. We use a cubic spline to interpolate between these nodes and obtain the full $w(z)$ in the redshift range $[0, z_{\max}]$. We set $z_{\max} = 1.0$ since the number and quality of SN Ia data, and hence constraints on dark energy, dramatically weaken beyond this redshift. At $z > z_{\max}$, we assume $w(z) = -1$. We have also tried allowing $w(z_{\max} \leq z \leq z_{CMB})$ to be a single new parameter free to vary; we found that the Markov chains do not converge because $w(z > z_{\max})$ is difficult to constrain using current data. Comparing this approach to setting this parameter as -1, we found that the best χ^2 remains nearly unchanged. Thus setting $w(z > z_{\max}) = -1$ is safe in the calculation. Overall, our parametrization of $w(z)$ can be summarized as:

$$w(z) = \begin{cases} -1, & z > z_{\max}; \\ w_i, & z \leq z_{\max}, z \in \{z_i\}; \\ \text{spline}, & z \leq z_{\max}, z \notin \{z_i\}. \end{cases} \qquad (2)$$

For the basic results, we choose $n = 6$ equation of state parameters (we discuss later the sensitivity to varying n).

It is important to take account of dark energy perturbations in the analysis, otherwise the results may be biased [3, 14]. In the conformal Newtonian gauge, one can derive the following perturbation equations [15]:

$$\dot{\delta} = -(1+w)(\theta - 3\dot{\Phi}) - 3\mathcal{H}(c_s^2 - w)\delta \qquad (3)$$

$$\dot{\theta} = -\mathcal{H}(1 - 3w)\theta - \frac{\dot{w}}{1+w}\theta + k^2\left(\frac{c_s^2}{1+w}\delta + \Psi\right) \qquad (4)$$

where the over-dot represents the derivative with respect to conformal time, $c_s^2 \equiv \delta P/\delta\rho$ is the sound speed, Ψ is the Newtonian potential, $\mathcal{H}$ is the (conformal time) Hubble parameter, δ is the density perturbation and θ the velocity perturbation. One easily sees that the perturbations δ and θ are divergent when $w(z)$ crosses -1 even if nothing in the physical model should diverge. One way to solve this problem is based on the quintom model [16] which we adopt here. In particular we introduce a small positive constant ϵ to divide the full range of the allowed values of w into three regions: I) $w > -1+\epsilon$; II) $-1+\epsilon \geq w \geq -1-\epsilon$; and III) $w < -1-\epsilon$. Neglecting the entropy perturbation contributions, for the regions I) and III) the equation of state does not cross -1 and the perturbations are well defined by solving Eq. (3) and (4).
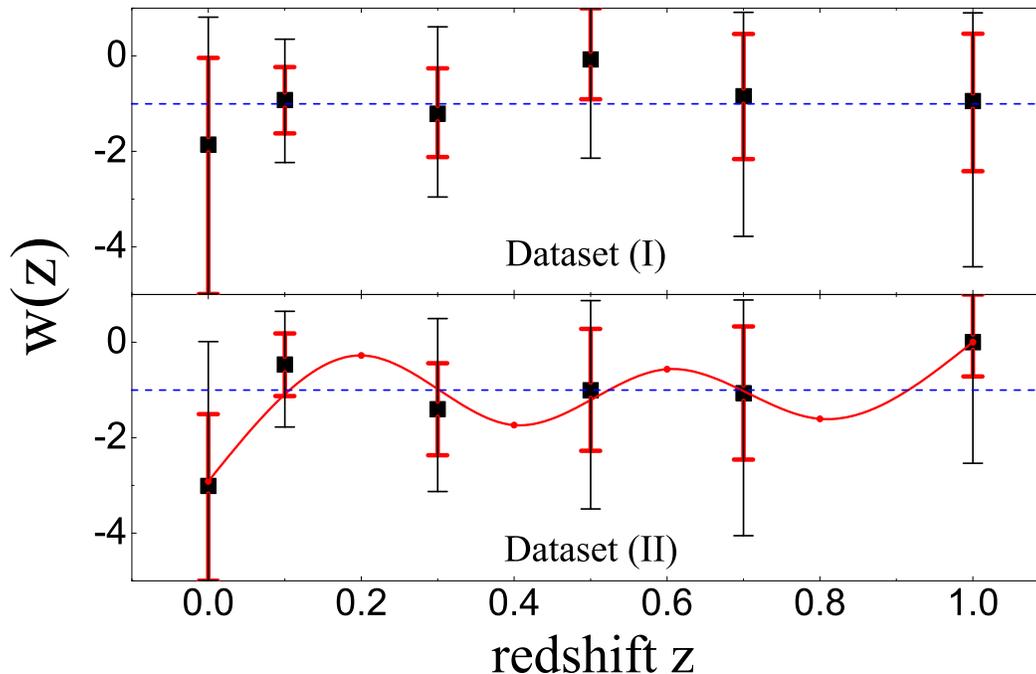
FIG. 1: Reconstruction of $w(z)$ using the datasets (I) (top panel) and (II) (bottom panel); see text for details. The red and black error bars correspond to 68 and 95% error bars respectively. ΛCDM model is shown with the blue dashed line. In the bottom panel, we also plot the reconstruction result with an alternative placement of fitting nodes (red points and curve; see the text for details).

For the region II), the density perturbation δ, the velocity perturbation θ, and their derivatives are finite and continuous for the realistic quintom dark energy models; therefore we set matching conditions in region (II), $\dot{\delta} = 0$ and $\dot{\theta} = 0$. This is an approximate method to calculate DE perturbation during crossing regime without introducing more parameters[1]. The error in this approximation is controllable and we have tested it in our numerical calculations; with $\epsilon \sim 10^{-5}$ we find that our method is a very good approximation to the two-field quintom dark energy model. For more details of this method we refer the reader to Refs. [3, 13].

In our calculations we take the total likelihood as the products of the separate likelihoods $(\mathcal{L}_i)$ of CMB, LSS and SN Ia, i.e. defining $\chi_i^2 \equiv -2 \log \mathcal{L}_i$, we use

$$\chi_{\text{total}}^2 = \chi_{\text{CMB}}^2 + \chi_{\text{LSS}}^2 + \chi_{\text{SNIa}}^2 . \qquad (5)$$

For the CMB data, we use the three-year WMAP (WMAP3) temperature-temperature and temperature-polarization power spectrum with the routine for computing the likelihood supplied by the WMAP team [18]. The LSS information we use consists of the galaxy power spectrum from the Sloan Digital Sky Survey (SDSS-gal; [19]); the luminous red galaxy power spectrum, also from the SDSS (SDSS-lrg; [20]) and the galaxy power spectrum from the 2dF Galaxy Redshift Survey (2dFGRS-gal; [21]). To be conservative, for all galaxy data we have used only the information at $k \leq 0.1h\,\text{Mpc}^{-1}$, corresponding to the linear regime. For SN Ia data, we use two datasets: Riess sample of 182 SNe [9] and ESSENCE sample of 192 SNe [22, 23]. We consider two dataset combinations:

(I) Riess-182+WMAP3+SDSS-gal+2dFGRS-gal;

(II) ESSENCE-192+WMAP3+SDSS-lrg+2dFGRS-gal.

In addition, for both datasets we also use the following information: Hubble Key Project measurement $H_0 = 72 \pm 8$ km s^{-1} Mpc^{-1}(1σ) [24]; baryon density information from the Big Bang Nucleosynthesis $\Omega_b h^2 =$

---

[1] Ref[17] has proved that in FRW cosmology, the equation of state of a single fluid or a single scalar field cannot cross -1. To realize such crossing, one has to introduce at least one more degree of freedom.

0.022 ± 0.002 (1σ) [25]; and a top-hat prior on the age of the universe, $10 \text{ Gyr} < t_0 < 20 \text{ Gyr}$.

For the MCMC calculation, we run eight independent chains each originally with $\mathcal{O}(10^5)$ elements, then thinned by a factor of 4. The average acceptance rate is about 50%. We ensure the convergence of the chains by Gelman and Rubin criteria [26] and find $R - 1 \sim \mathcal{O}(10^{-2})$ which is more conservative than the recommended value $R - 1 \sim \mathcal{O}(10^{-1})$.

Results. We first study how the results change as we vary the number of and location of fitting nodes describing $w(z)$. We start out by placing one fitting node each at $z = 0$ and $z = z_{\max} = 1$, then increase n, adding fitting nodes so that they are uniformly spaced in redshift; $z_i = (i-1)/(n-1), (n \geq 2, \ n \in \mathbb{N})$. For each n and using the dataset (II), we calculate the improvement in χ^2 relative to the ΛCDM model, $\Delta\chi^2 = \chi^2_{\min} - \chi^2_{\Lambda\text{CDM}}$. As expected, we find that $n = 2$ already has a better fit than the ΛCDM model, and the fit improves as n is increased. When n is greater than 6, however, $\Delta\chi^2$ flattens off (see panel (F) of Fig. 2). We therefore conclude that the data we use have enough power to constrain 6 equation of state parameters. Therefore, at least when $n \leq 8$ is considered, $n = 6$ is the optimal choice since a higher n does not improve the fit[2].

We also test the prescription of how to place the fitting nodes in redshift in the lower panel of Fig. 1. The black points with error bars are for placement $z_i \in \{0, 0.1, 0.3, 0.5, 0.7, 1.0\}$; the red points with red curve are for placement $z_i \in \{0, 0.2, 0.4, 0.6, 0.8, 1.0\}$. We see that the red curve almost coincides with the black points, namely, the dependence of result on placement of fitting nodes is weak. The above test and analysis has been also done with dataset (I) and a similar result is found. In what follows, we adopt the former, slightly non-uniform placement in redshift.

Given the above two cosmological datasets, we explore the 12-D parameter space from Eq. (1). After marginalizing over other cosmological parameters, we obtain the constraint of DE parameters w_i as plotted in Fig. 1. In the upper panel, we find that almost all the mean values of points are consistent with the prediction of ΛCDM model except for the 1st and the 4th points, at redshifts 0 and 0.5. The equation of state at the present epoch is slightly favored to be below -1, while the equation of state at redshift 0.5 is greater than -1 at 68% C.L., showing a small "bump". This bump most likely stems from a feature in the Hubble diagram of the Riess-182 dataset (I). To see this, we replace the Riess-182 and SDSS-gal data by ESSENCE-192 and SDSS-lrg data respectively and get the result in lower panel of Fig. 1. With this new dataset, the bump at redshift 0.5 disappears and

---

[2] We are aware of that the fit must further improve for some higher n because *any* dataset can be perfectly fit by some suitable, but possibly highly oscillatory, $w(z)$.

$w(0.1 \lesssim z \lesssim 0.9)$ is consistent with -1 at 68% C.L.. The equation of state at redshifts 0 and 1 deviates from -1, but not significantly.

The equation of state parameters w_i are correlated, however, somewhat complicating their interpretation; for example, the highest correlation coefficient is -0.9, between w_4 and w_5. It is therefore useful to de-correlate the w_i, as done in Ref. [7].

For each MCMC run, we compute the covariance matrix of the equation-of-state parameters, $\mathbf{C} = (w_i - \langle w_i \rangle)(w_j - \langle w_j \rangle)^T \equiv \langle \mathbf{p}\mathbf{p}^T \rangle$, using CosmoMC [12]. We then diagonalize the Fisher matrix $\mathbf{F} \equiv \mathbf{C}^{-1}$, so that $\mathbf{F} = \mathbf{O}^T \mathbf{D} \mathbf{O}$; here $\mathbf{O}$ is the resulting orthogonal matrix and $\mathbf{D}$ is diagonal.

One can now rotate the parameters into a basis where the new parameters $\mathbf{q}$ are uncorrelated; $\mathbf{q} = \mathbf{W}\mathbf{p}$. There are many ways to do so [27]. Here we make two alternative choices.

Choice 1: $\mathbf{W}_1 = \mathbf{F}^{1/2}$; then
$$\mathbf{C}_{\mathbf{q}_1} = \langle \mathbf{q}_1 \mathbf{q}_1^T \rangle = \mathbf{W}_1 \langle \mathbf{p}\mathbf{p}^T \rangle \mathbf{W}_1^T = \mathbf{I}.$$

Choice 2: $\mathbf{W}_2 = \mathbf{O}$; then
$$\mathbf{C}_{\mathbf{q}_2} = \langle \mathbf{q}_2 \mathbf{q}_2^T \rangle = \mathbf{W}_2 \langle \mathbf{p}\mathbf{p}^T \rangle \mathbf{W}_2^T = \mathbf{D}^{-1}.$$

Here $\mathbf{W}_1$ corresponds to the localized principal component (heretofore LPC) decomposition of the parameters $\mathbf{p}$ — the weights (rows of $\mathbf{W}_1$) are almost positive definite and fairly well localized in redshift [7]. $\mathbf{W}_1$ is usually rescaled so that its rows sum up to unity, $\sum_{j=1}^{n} (\mathbf{W}_1)_{ij} = 1$, and we follow this practice. Note, however, that the physical inferences do not depend on the normalization of $\mathbf{W}_1$ (or $\mathbf{W}_2$) as both the parameters $\mathbf{q}$ and their values for a particular theoretical model change consistently. For example, we have tried a different normalization of $\mathbf{W}_1$ and explicitly checked that the parameters $\mathbf{q}$ and their values corresponding to the $w(z) = -1$ model change so that the hypothesis test of whether the measured parameters are consistent with $w(z) = -1$ returns the same result.

We find that all LPC band powers are consistent with the cosmological constant value at 95% C.L. Two out of six points deviate from ΛCDM at greater than 68% C.L, which is not statistically unexpected. This conclusion is easy to read off in the panel (A) of Fig. 2 where the $\mathbf{q}$'s are uncorrelated, and is independent of the choice of the decorrelating weights. In panel (C), we replace $\mathbf{q}_1$ with $\mathbf{q}_2$ (with $\mathbf{W}_2$ normalized as $\mathbf{W}_1$ above), and again find consistency with the cosmological constant scenario.

Summary and Discussion. Using the latest astronomical data of SNe Ia, CMB and LSS, we used the MCMC machinery to reconstruct the expansion history of the universe, and the evolution of dark energy, in a nearly model-independent fashion. We used the cubic spline interpolation between n values of the equation state w_i, fitting the expansion history more flexibly than essentially any description used on existing data so far. We found that $n = 6$ values of the equation of state in the range $0 \leq z \leq 1$ can be usefully constrained, and that increasing their number slightly does not improve the fit.
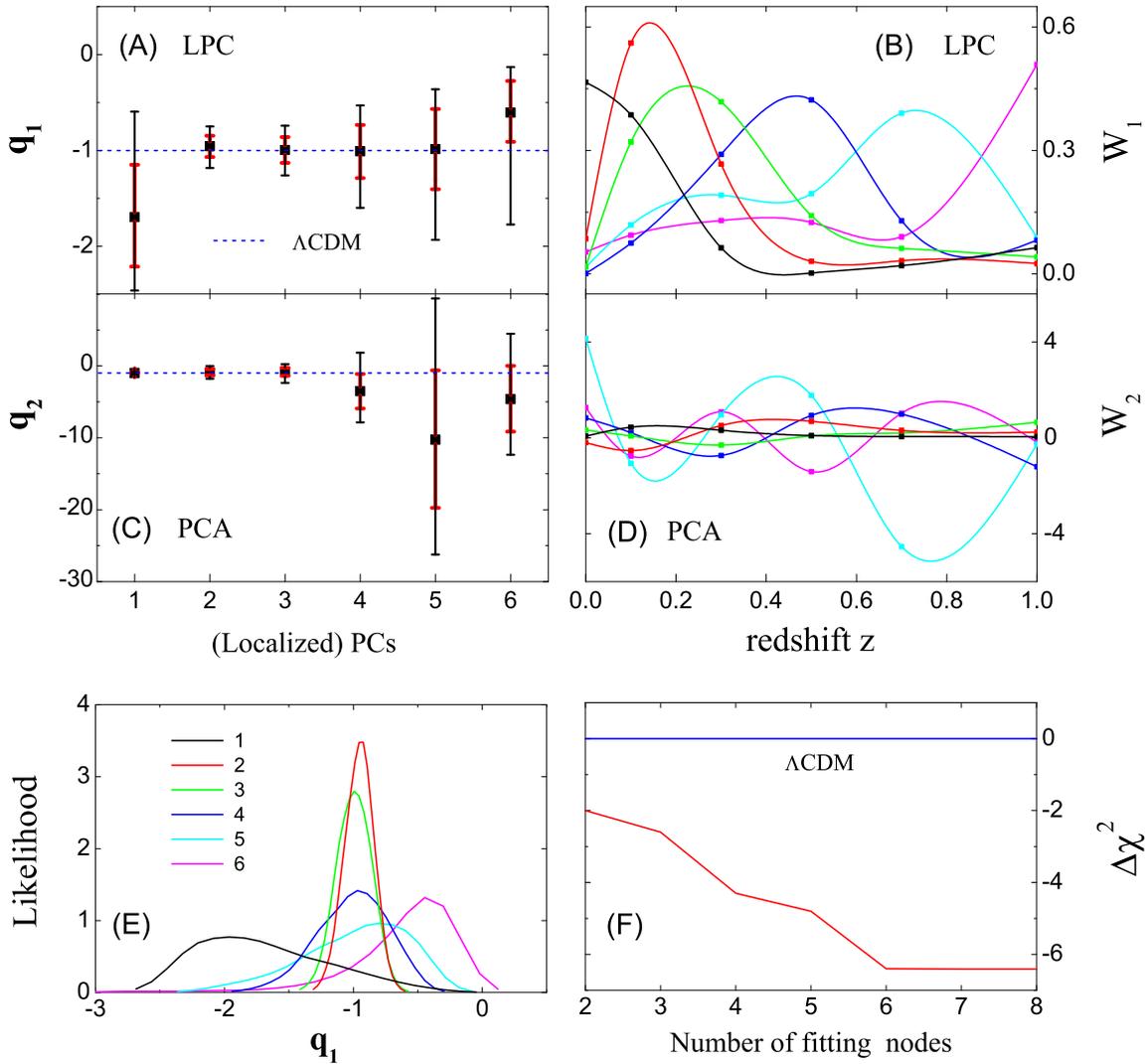
FIG. 2: Constraints on uncorrelated band powers of the equation of state $w(z)$, using the dataset II. Panels (A) and (B) show the median values and the 68% and 95% constraints on the localized principal components $\mathbf{q}_1$, and their weights in redshift $\mathbf{W}_1$, respectively. Panels (C) and (D) show the same for the principal components $\mathbf{q}_2$ and their weights $\mathbf{W}_2$ (see the text for definitions). Panel (E) shows the likelihood distributions for the parameters $\mathbf{q}_1$, while panel (F) shows the reduction in χ^2 relative to ΛCDM as the number of fitting nodes (for parameters $\mathbf{q}_1$) is increased.

Some comments can be made about our approach. We think the cubic spline leads a largely unbiased reconstruction of $w(z)$. An exception to this would be a highly oscillatory fiducial $w(z)$, which however cannot be robustly constrained with other approaches (and current data) either. Moreover, our results are not in conflict with Ref. [28] who claimed that only 2-3 equation-of-state parameters can be measured even from future surveys to better than about 10%, since we do not measure the six w_i to nearly such a good accuracy; see Fig. 1. Finally,

one could certainly apply the same approach to the reconstruction of the dark energy density $\rho_{\mathrm{DE}}(z)$ as in [29], although we would argue that probing dynamics of dark energy requires specifically $w(z)$.

Our results do not show any significant evidence for the evolution of the equation of state with time, and are fully consistent with the cosmological constant scenario in the interval $0 \leq z \leq 1$ at the 95% C.L. We would particularly like to be able to test the dynamics of dark energy; for example, the "freezing" and "thawing" scalar

field models [30] which have different physical behavior and a different sign of dw/dz; however the accuracy we have right now is not sufficient to distinguish between these models [31]. Our method is straightforward to implement, and will produce sharp tests of the dynamics of dark energy once we have data from the next-generation surveys, such as Dark Energy Survey [32], Joint Dark Energy Mission [33], Large Synoptic Sky Telescope [34], and Pan-STARRs [35].

[1] A. R. Cooray and D. Huterer, Astrophys. J. **513**, L95 (1999); P.S. Corasaniti and E.J. Copeland, Phys. Rev. D **67** 063521 (2003); T.R. Choudhury and T. Padmanabhan, MNRAS, **344**, 823 (2003); E.V. Linder, Phys. Rev. Lett. **90**, 091301 (2003); M. Chevallier and D. Polarski, Int. J. Mod. Phys. D **10**, 213 (2001); U. Alam *et al.*, MNRAS **344**, 1057 (2003).
[2] A. Melchiorri, L. Mersini-Houghton, C.J. Odman and M. Trodden, Phys. Rev. D **68** 043509 (2003); S. Hannestad and E. Mortsell, JCAP **0409**, 001 (2004); S. Nesseris, L. Perivolaropoulos, Phys. Rev. D **72** 123519 (2005); M. Jarvis, B. Jain, G. Bernstein and D. Dolney, Astrophys. J. **644**, 71 (2006); A. Liddle, P. Mukherjee, D. Parkinson and Y. Wang, Phys. Rev. D **74** 123506 (2006).
[3] J. Q. Xia, G. B. Zhao, B. Feng, H. Li and X. Zhang, Phys. Rev. D **73**, 063521 (2006); G. B. Zhao, J. Q. Xia, B. Feng and X. Zhang, Int. J. Mod. Phys. D **16**, 1229 (2007); G. B. Zhao, J. Q. Xia, H. Li, C. Tao, J. M. Virey, Z. H. Zhu and X. Zhang, Phys. Lett. B **648**, 8 (2007).
[4] U. Alam, V. Sahni and A. A. Starobinsky, JCAP **0702**, 011 (2007).
[5] J. Q. Xia, H. Li, G. B. Zhao and X. Zhang, arXiv:0708.1111; G. B. Zhao, J. Q. Xia and X. M. Zhang, JCAP **0707**, 010 (2007); J. Q. Xia, G. B. Zhao and X. Zhang, Phys. Rev. D **75**, 103505 (2007).
[6] P.S. Corasaniti, M. Kunz, D. Parkinson, E.J. Copeland, and B.A. Bassett, Phys. Rev. D **70** 083006 (2004); Y. Wang and M. Tegmark, Phys.Rev.Lett. **92**, 241302 (2004); Y. Wang and P. Mukherjee, Astrophys. J. **606**, 654 (2004); A. Shafieloo, U. Alam, V. Sahni and A.A. Starobinsky, MNRAS **366**, 1081 (2006); C. Zunckel and R. Trotta, MNRAS **380**, 865 (2007).
[7] D. Huterer and A. Cooray, Phys. Rev. D **71**, 023506 (2005).
[8] Y. Wang and M. Tegmark, Phys. Rev. D **71**, 103513 (2005).
[9] A. G. Riess *et al.*, arXiv:astro-ph/0611572.
[10] D. Huterer and G. Starkman, Phys. Rev. Lett. **90**, 031301 (2003); R. G. Crittenden and L. Pogosian, arXiv:astro-ph/0510293.
[11] R. de Putter and E. V. Linder, arXiv:0710.0373.
[12] A. Lewis and S. Bridle, Phys. Rev. D **66**, 103511 (2002).
[13] G. B. Zhao, J. Q. Xia, M. Li, B. Feng and X. Zhang, Phys. Rev. D **72**, 123515 (2005).
[14] J. Weller and A. M. Lewis, Mon. Not. Roy. Astron. Soc. **346**, 987 (2003); C. Yeche, A. Ealet, A. Refregier, C. Tao, A. Tilquin, J. M. Virey and D. Yvon, arXiv:astro-ph/0507170.
[15] C. P. Ma and E. Bertschinger, Astrophys. J. **455**, 7 (1995).
[16] B. Feng, X. L. Wang and X. M. Zhang, Phys. Lett. B **607**, 35 (2005).
[17] J. Q. Xia, Y. F. Cai, T. T. Qiu, G. B. Zhao and X. Zhang, arXiv: astro-ph/0703202.
[18] D. N. Spergel *et al.*, Astrophys. J. Suppl. **170**, 377 (2007).
[19] M. Tegmark *et al.*, Astrophys. J. **606**, 702 (2004).
[20] M. Tegmark *et al.*, Phys. Rev. D **74**, 123507 (2006).
[21] S. Cole *et al.*, Mon. Not. Roy. Astron. Soc. **362** (2005) 505.
[22] G. Miknaitis *et al.*, Astrophys. J. **666**, 674 (2007).
[23] T. M. Davis *et al.*, Astrophys. J. **666**, 716 (2007).
[24] W. L. Freedman *et al.*, Astrophys. J. **553**, 47 (2001).
[25] S. Burles, K. M. Nollett and M. S. Turner, Astrophys. J. **552**, L1 (2001).
[26] A. Gelman and D. Rubin, Statistical Science **7**, 457 (1992).
[27] A.J.S. Hamilton and M. Tegmark, MNRAS **312**, 285 (2000).
[28] D. Huterer and E. V. Linder, Phys. Rev. D **72**, 043509 (2005).
[29] Y. Wang and P. Mukherjee, Astrophys. J. **650**, 1 (2006).
[30] R.R. Caldwell and E. V. Linder, Phys. Rev. Lett **95**, 141301 (2005).
[31] D. Huterer and H. V. Peiris, Phys. Rev. D **75**, 083503 (2007).
[32] http://www.darkenergysurvey.org
[33] http://universe.nasa.gov/program/probes/jdem.html
[34] http://www.lsst.org/lsst_home.shtml
[35] http://pan-starrs.ifa.hawaii.edu/public/